

# Electricity Generation from Heavy Metal-Containing Wheat Grain Hydrolysate Using Single-Chamber Microbial Fuel Cells: Performance and Long-Term Stability

Guang-En Yuan, Honghu Deng, Xiangli Ru, Xin Zhang\*

School of Environment, Henan Normal University, Key Laboratory for Yellow River and Huai River Water Environmental and Pollution Control, Ministry of Education, Henan Key Laboratory for Environmental Pollution Control, Xinxiang, Henan 453007, PR China.

\*E-mail: [xinzhang2015@126.com](mailto:xinzhang2015@126.com)

Received: 12 June 2018 / Accepted: 4 July 2018 / Published: 5 August 2018

---

In this study, heavy metal-containing wheat grain (HMWG) hydrolysate was explored as a potential fuel in membrane-less single chamber microbial fuel cells (MFCs) for electricity production. The maximum coulombic efficiency got up to 15.7%, and the corresponding removal rate of chemical oxygen demand was 83.4%. A maximum power density of 381 mW/m<sup>2</sup> was achieved with relatively low concentration of the HMWG hydrolysate, but high concentration of the HMWG hydrolysate restrained the electricity production in a MFC, especially after long-terms of operation. The results of electrochemical analysis and scanning electron microscope proved that the decreased performance in electricity generation was mainly ascribed to the declined electrocatalytic activities of the MFC anode and the attenuated microorganisms on its surface. The present work demonstrates that attention should be paid to the toxicity of heavy metals in energy recovery from heavy metal-containing organic wastes by MFCs.

---

**Keywords:** Microbial fuel cell; Heavy metal; Organic waste; Electricity generation; Long-term stability

## 1. INTRODUCTION

Anthropogenic activities, such as fossil fuel combustion, mining, smelting, traffic, wastewater irrigation and sewage sludge reuse, can cause heavy metal pollution in farmland, which has become an increasingly serious problem for modern agriculture [1]. Soil-bound heavy metals in farmlands are likely to accumulate in agricultural products, e.g. leafy vegetables and cereal grains, which pose risks

to human population which consume the polluted agricultural food or indirectly consume animals feeding on the agricultural products via the food chain [2-4]. These vegetables and grains compose of many valuable components, such as starch, protein, cellulose and hemicellulose, which contain a huge amount of potential energy. Methane production by anaerobic digestion from crop residues containing heavy metals was explored in a laboratory-scale continuous stirred-tank reactor [5]. However, only about 30–40% of the methane energy can be converted into electricity, and the remainder is given off as heat [6]. Rational utilization and disposal of the heavy metal-containing agricultural biomass should be put on the agenda.

Microbial fuel cells (MFCs) are innovative energy-converting systems that can produce electric energy directly from organic or inorganic matter [7, 8]. In such devices, electro-active microorganisms acting as biocatalyst extract electrons from substrate and transfer them onto the anode. These electrons then travel through an external circuit to the cathode, where they react with the final electron acceptors (such as oxygen or nitrate). A wide range of biodegradable substances can be used as fuels in a MFC, such as glucose [9], cellulose [10], proteins [11] and domestic wastewaters [12], making it a promising technology for waste treatment due to the simultaneous energy recovery.

Agricultural biomass can be also used as fuel materials in MFCs for electricity generation due to their high content of carbohydrates. Rapeseed straw treated by combination of hydrothermal pretreatment and enzymatic hydrolysis was utilized as a fuel in two-chamber MFCs for electrical power generation, and the power density reached 54 mW/m<sup>2</sup> [13]. MFC fed with cornstalk hydrolysate obtained by hydrothermal liquefaction method achieved a maximum power density of 680 mW/m<sup>3</sup> [14]. Pristine agricultural biomass without pretreatment, such as rice straw [15], corncob pellets [16] and orange peel waste biomass [17], have also been tested as substrates in MFCs. Although the power densities achieved are relatively low currently, MFCs hold great potential in extracting energy from agricultural biomass. To our knowledge, there is no relative report focusing on heavy metal-containing agricultural biomass for electricity generation in MFCs, and the performance and long-term stability of MFCs remain to be explored.

The objectives of this study were to (1) investigate the feasibility of heavy metal-containing wheat grain (HMWG) hydrolysate as a potential fuel in MFCs for electricity production and (2) evaluate the long-term stability of these MFC reactors.

## 2. METHODS

### 2.1. Preparation of the HMWG hydrolysate

HMWG was obtained from a sewage irrigation area in Henan province of China. The grain was washed with deionized water, dried in an air dry oven and ground into powder successively. The HMWG hydrolysate was obtained by liquidation of the powder, and the operation procedure are described briefly as follows. Twenty five grams of the powder was put into deionized water of 500 mL and mixed on a constant temperature magnetic stirrer. The temperature of the mixture was maintained at 73 ± 2 °C for 30 min, 90 ± 2 °C for 20 min and 70 ± 2 °C for 20 min successively. Subsequently, 0.5

gram of  $\alpha$ -amylase was put into the mixture and agitation was kept for another half an hour. After cooling down, the mixture was filtered with rapid filter paper. The filtrate was collected into a serum bottle and stored in a refrigerator at 4 °C before being used. Characteristics of the HMWG hydrolysate are shown in Table 1.

**Table 1.** Characteristics of the HMWG hydrolysate

Parameter	Value
Chemical oxygen demand (COD, g/L)	42.752 ± 0.89
Soluble polysaccharide (g/L)	22.03 ± 0.74
Total Kjeldahl nitrogen (g/L)	1.17 ± 0.43
Pb (µg/L)	6.38
Cr (µg/L)	137
Ni (µg/L)	19.1
Fe (µg/L)	145
Cu (µg/L)	36.9
Zn (µg/L)	53.6
Cd (µg/L)	1.66
As (µg/L)	6.22

## 2.2. Microbial fuel cell construction and operation

The membrane-less single chamber MFC reactors were constructed by a rectangular Perspex with 4 cm long by 3 cm in diameter. Each of the MFC reactors (28 mL) was consisted of graphite fiber brush (2.5 cm diameter × 2.5 cm length) as anode and carbon paper containing 0.5 mg/cm<sup>2</sup> Pt catalyst as cathode (surface area of 7 cm<sup>2</sup>). Graphite fiber brushes were washed firstly in acetone and then 1 M hydrochloric acid to remove organic impurity and metals from the surface before installation. The other side of carbon paper cathodes faced to air were wet-proofed by carbon powder and polytetrafluoroethylene.

Six MFC reactors were started up and operated in fed-batch mode at a fixed external resistance of 1000 Ω, and refilled each time the voltage decreased below 50 mV. The MFC reactors were all inoculated with secondary sludge from a municipal wastewater treatment plant (Xinxiang, China) and a phosphate buffered solution (PBS) containing 0.75 g/L glucose. The PBS solution contained: NH<sub>4</sub>Cl (0.31 g/L); NaH<sub>2</sub>PO<sub>4</sub>·H<sub>2</sub>O (19.88 g/L); Na<sub>2</sub>HPO<sub>4</sub>·H<sub>2</sub>O (11 g/L); KCl (0.13 g/L), and a metal (12.5 mL) and vitamin (5 mL) solution [18]. When steady and repeatable voltage cycles were achieved, the MFC reactors were divided into three groups (two reactors in one group), which were named as MFC-1, MFC-2, MFC-3 and their duplicates. Then, the electrolytes of the three reactor groups (from MFC-1 to MFC-3) were changed into the HMWG hydrolysate with 40, 20, and 10 times dilution by the PBS solution. The reactor electrolytes were all sparged with high purity nitrogen gas for at least 20 min to eliminate dissolved oxygen and the pH adjusted to 7.0 before injected into the MFC reactors. All

experiments were conducted at an ambient room temperature ( $20 \pm 3$  °C), and the average values were reported.

### 2.3. Analytical methods and calculations

Cell voltages across the external resistance were continuously recorded every 30 min by a data acquisition system (PISO-813, Hongge Taiwan). Coulombic efficiency (CE), a parameter indicating the fraction of electrons transferred to the anode derived from the substrate, was calculated according to the method of [19]. The polarization curves were obtained by changing external circuit resistances from 10000 to 50  $\Omega$  during the steady state. A saturated calomel electrode (SCE, 241 mV vs standard hydrogen electrode; SHE) was inserted into the electrolyte to measure anode and cathode potentials by using a multimeter (VC8246B, China). Current density was calculated as  $I = U/RA$ , where  $U$  (V) is the voltage,  $R$  ( $\Omega$ ) the external resistance, and  $A$  ( $m^2$ ) the projected area of the MFC cathode. Power density ( $mW/m^2$ ) was calculated as  $P = UI$ , and the internal resistance ( $R_{in}$ ) of the MFC reactor was calculated by the power density peak method [20]. COD and Total Kjeldahl nitrogen measurements were conducted using standard methods [21]. Soluble polysaccharide was determined by the phenol-sulfuric method with glucose as the standard. After digestion, the metals were analyzed by inductively coupled plasma–mass spectrometry (ELAN DRC-e, America Perkin Elmer).

All electrochemical experiments were performed using an electrochemical workstation (CHI660E, Shanghai Chenhua Instruments Co., Ltd.) after the MFC reactor was refilled and its open-circuit voltage got stable. Cyclic voltammetry (CV) and Tafel tests were conducted to study electrochemical behavior of the anode biofilms in a three-electrode system consisting of a working electrode (anode), a counter electrode (cathode) and a SCE reference electrode at a scan rate of 1 mV/s. All potentials shown in this study were corrected to a SHE. The Tafel equation described the relationship between the anodic overpotential and the current density in the high overpotential region, which was expressed as Eq. (1):

$$\eta_{an} = \frac{RT}{\beta F} \lg \left( \frac{i}{i_0} \right) \quad (1)$$

where  $\eta_{an}$  was the anodic overpotential (V),  $R$  the ideal gas constant (8.31 J/mol K),  $T$  the temperature (K),  $F$  the Faraday constant (96,485 C/mole<sup>-1</sup>),  $\beta$  the symmetry factor (a constant reflecting the change of activation energy with anode potential),  $i$  the current density and  $i_0$  the exchange current density, a variable parameter related to the activation energy of anodic reduction under equilibrium conditions.

The tests of polarization, CV and Tafel curves were conducted after 10 and 55 days of operation with the HMWG hydrolysate as the fuel, respectively. After the experiments finished, the morphology of biofilms on the anode surface was characterized by scanning electron microscope (SEM). The biofilm samples for SEM characterization were prepared as follows: (a) samples were fixed by 5 wt.% glutaric aldehyde in 50 mM phosphate buffer solution (pH = 7.0); (b) samples were dehydrated in a graded series of ethanol aqueous solution (10%, 25%, 40%, 55%, 70%, 80%, 90% and

100%) then were taken out and naturally dried at room temperature; (c) samples were coated with gold and examined under a field emission SEM (SU8010, Japan).

### 3. RESULTS

#### 3.1. Voltage outputs of the MFC reactors

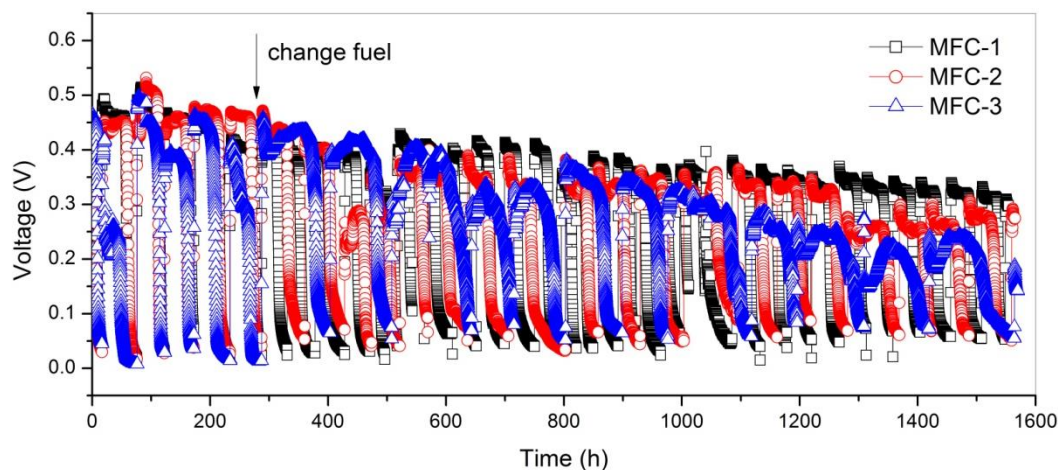


**Figure 1.** Voltage outputs of the MFC reactors as a function of time

Glucose was used as a fuel for the start up of MFCs because the main components of the HMWG hydrolysate was carbohydrates. Fig. 1 shows the voltage outputs of the MFC reactors with different concentrations of the HMWG hydrolysate as a function of time. When glucose as the fuel, stable voltage outputs of  $0.47 \pm 0.12$  V were obtained for all MFCs. No obvious drop of voltage outputs was observed for the three MFCs in the first batch after changing the fuel, but all voltage outputs gradually decreased afterwards. MFC-3 with higher concentration (10 times dilution) of the HMWG hydrolysate obtained a voltage output of  $0.2 \pm 0.04$  V after 55 days of operation, which was lower than that of MFC-1 (40 times dilution,  $0.34 \pm 0.07$  V) and MFC-2 (20 times dilution,  $0.28 \pm 0.06$  V). The COD removal rates, CEs and average batch times of the MFC reactors in the first three batches after changing fuel are shown in Table 2.

**Table 2.** The COD removal rates, CEs and average batch times of the MFC reactors in the first three batches after changing the fuel

Reactor	Dilution ratio	Influent COD (mg/L)	COD removal rate (%)	CE (%)	Average batch time (h)
MFC-1	40 ×	$1244.5 \pm 10.7$	$83.4 \pm 3.7$	$15.7 \pm 1.5$	$47.1 \pm 2.7$
MFC-2	20 ×	$2622.3 \pm 64.7$	$83.9 \pm 1.3$	$14.3 \pm 0.9$	$70.6 \pm 2.4$
MFC-3	10 ×	$5410.2 \pm 77.3$	$90.3 \pm 4.2$	$11.5 \pm 0.9$	$110.3 \pm 5.7$

Values are given as mean values  $\pm$  standard deviation ( $n = 3$ ).

The COD removal rates for MFC-1 and MFC-2 were comparative but lower than that for MFC-3, which may be due to the higher concentration of the HMWG hydrolysate in MFC-3. However, MFC-3 obtained a CE of  $11.5 \pm 0.9\%$ , which was lower than MFC-1 ( $15.7 \pm 1.5\%$ ) and MFC-2 ( $14.3 \pm 0.9\%$ ).

### 3.2. Polarization and power curves

Polarization and power density curves were obtained to evaluate the power generation of the MFCs. After 10 days of operation with the HMWG hydrolysate as the fuel (Fig. 2a), MFC-3 achieved an open-circuit potential (OCP) of 0.615 V, which was higher than that for MFC-1 (0.606 V) and MFC-2 (0.531 V).

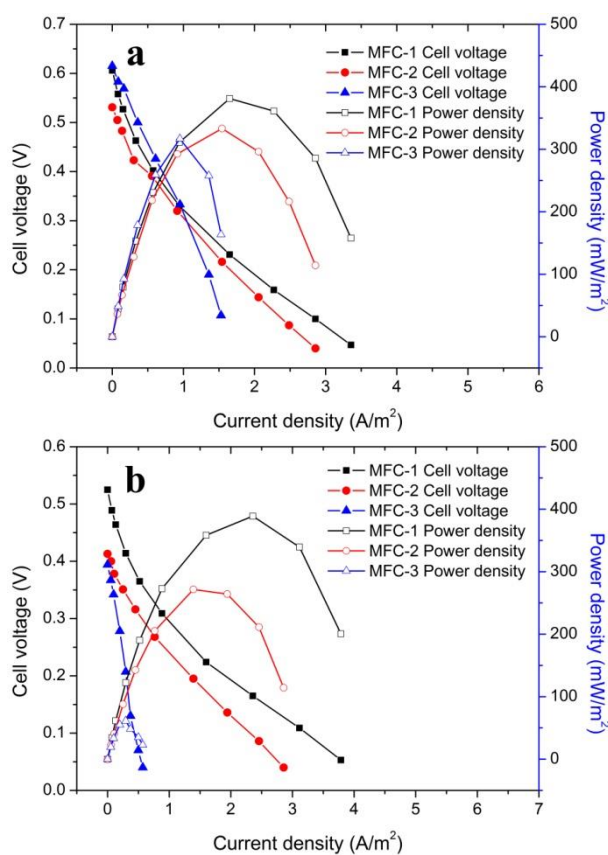


**Figure 2.** Polarization and power density curves of the MFCs after 10 (a) and 55 (b) days of operation with the HMWG hydrolysate as the fuel

The electric powers generated by MFCs, however, were not proportional to the concentration of the fuel. MFC-3 produced a maximum power density (MPD) of  $317 \text{ mW/m}^2$  at the current density of  $0.95 \text{ A/m}^2$ , which was lower than that for MFC-1 ( $381 \text{ mW/m}^2$ ) and MFC-2 ( $333 \text{ mW/m}^2$ ). The  $R_{in}$  for MFC-3 was calculated as  $501 \Omega$ , higher than that for MFC-1 ( $200 \Omega$ ) and MFC-2 ( $200 \Omega$ ). After 55

days of operation with the HMWG hydrolysate as the fuel (Fig. 2b), the OCPs for MFC reactors (from MFC-1 to MFC-3) decreased to 0.525, 0.413 and 0.394 V, which were 13.4%, 22.2% and 35.9% lower than those obtained after 10 days of operation, respectively. The MPD of MFC-1 was  $389 \text{ mW/m}^2$ , a little higher than that obtained after 10 days of operation. This could be attributed to the adaptation and evolution of microbial communities after changing fuel, resulting in a lower  $R_{in}$  of  $100 \Omega$ . The MPD and  $R_{in}$  of MFC-2 were  $389 \text{ mW/m}^2$  and  $200 \Omega$ , respectively. MFC-3 obtained a MPD of  $61 \text{ mW/m}^2$ , 80.8% lower than that obtained after 10 days of operation, and its  $R_{in}$  increased from 501 to  $999 \Omega$ .

The anode and cathode polarization curves of the three MFCs were obtained to evaluate the discharge performance and stability of individual electrode.

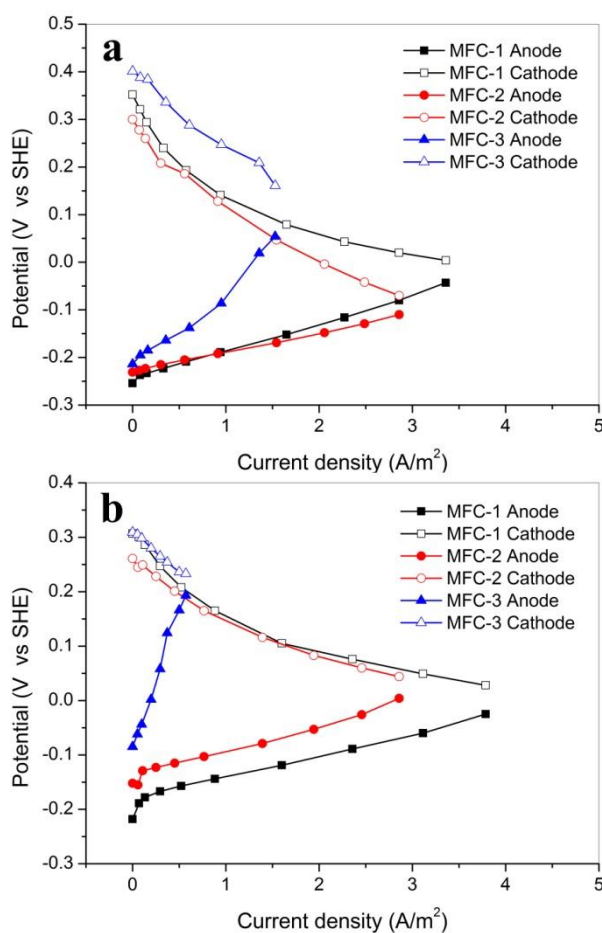


**Figure 3.** The anode and cathode polarization curves of the MFCs after 10 (a) and 55 (b) days of operation with the HMWG hydrolysate as the fuel

After 10 days of operation with the HMWG hydrolysate as the fuel (Fig. 3a), MFC-3 possessed a cathode polarization curve above MFC-1 and MFC-2 obviously, demonstrating that the poor performance of MFC-3 in electricity generation was due to the performance of the anode and not the cathode. The OCPs of the three MFC anodes (from MFC-1 to MFC-3) were  $-0.254$ ,  $-0.231$  and  $-0.214$  V, but the anode polarization curve of MFC-3 showed a higher slope value than those of the other two MFCs. For MFC-3, the anode potential varied to  $0.054$  V at the maximum current density of  $1.53 \text{ A/m}^2$ . This indicates that higher concentration of the HMWG hydrolysate would suppress the

electrochemical activity of the MFC anode. After 55 days of operation with the HMWG hydrolysate as the fuel (Fig. 3b), it was observed that the performances of the three MFC cathodes all decreased, but MFC-3 still possessed a cathode polarization curve above MFC-1 and MFC-2. The OCPs of the MFC anodes (from MFC-1 to MFC-3) reduced to  $-0.218$ ,  $-0.152$  and  $-0.085$  V, respectively. The anode potential of MFC-3 changed to  $0.193$  V at the maximum current density of  $0.57$  A/m<sup>2</sup>. These results demonstrated that the concentration of the HMWG hydrolysate had an important effect on the long-term stability of the MFC anode.

### 3.3. Electrochemical properties of the MFC anodes

CV tests were conducted to investigate the bioelectrocatalytic activities of the anode biofilms. After 10 days of operation with the HMWG hydrolysate as the fuel (Fig. 4a), an increasing current was found in all CV curves in the oxidation scan, and their magnitude followed the order of MFC-1 > MFC-2 > MFC-3.

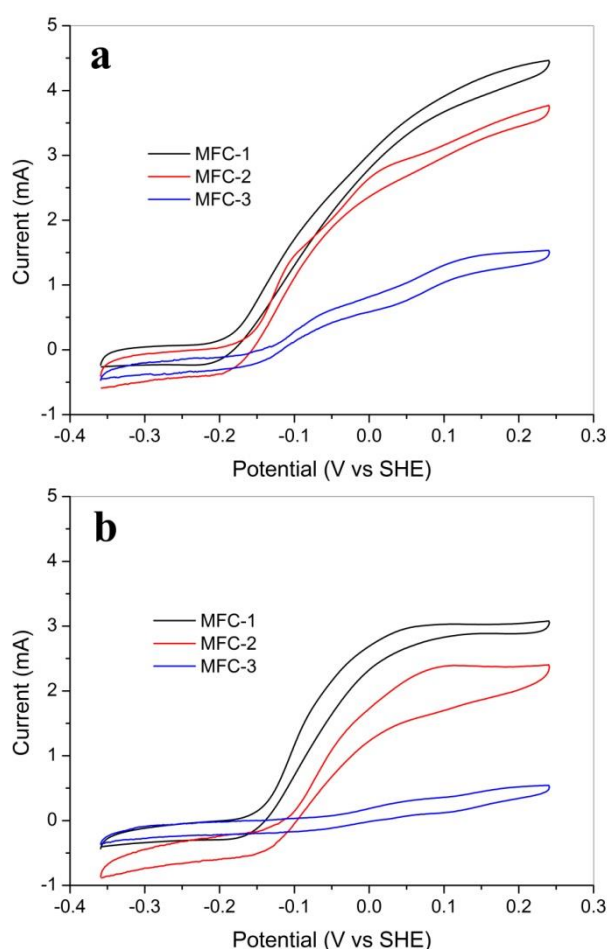


**Figure 4.** CV curves of the MFC anodes after 10 (a) and 55 (b) days of operation with the HMWG hydrolysate as the fuel

Particularly, MFC-3 obtained a maximum current of  $1.30$  mA at the potential of  $0.2$  V, which was much lower than MFC-1 ( $4.13$  mA) and MFC-2 ( $3.45$  mA) at the same potential. This indicates that the anode biofilm of the MFC-3 had a lower bioelectrocatalytic activity than the other two

reactors. After 55 days of operation with the HMWG hydrolysate as the fuel (Fig. 4b), all CV curves reached a plateau at the relatively positive potentials, which were different from the ones obtained after 10 days of operation. The maximum currents of the three MFCs (from MFC-1 to MFC-3) in the oxidation scans were 3.04, 2.38 and 0.52 mA, respectively. These decreased currents demonstrated that the bioelectrocatalytic activities of the anode biofilms all declined after long-term operation.

Tafel curves provide valuable information about activation loss and help to interpret the biocatalytic activity based on the derived kinetic parameters, in the form of exchange current density ( $i_0$ ) and Tafel slope ( $RT/\eta F$ ) [22]. Based on the Tafel equation, the Y-axis intercept is the logarithm of the exchange current densities ( $\lg i_0$ ). The Tafel curves (Fig. 5) were fitted reasonably well ( $R^2 \geq 0.998$ ) at the overpotential of 60–80 mV, where  $|F\eta/RT| > 1$  [23, 24].

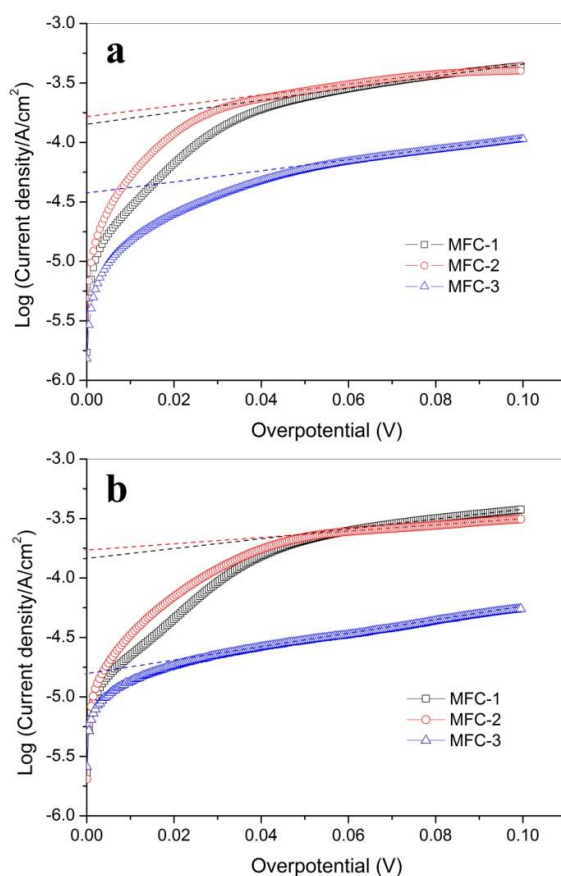


**Figure 5.** Tafel plots of the MFC anodes after 10 (a) and 55 (b) days of operation with the HMWG hydrolysate as the fuel

The exchange current densities and anodic slopes of the MFCs obtained from Tafel curves were showed in Table 3. After 10 days of operation with the HMWG hydrolysate as the fuel (Fig. 5a), MFC-3 got a exchange current density of  $0.038 \text{ mA/cm}^2$ , which was much lower than those of MFC-1 ( $0.133 \text{ mA/cm}^2$ ) and MFC-2 ( $0.172 \text{ mA/cm}^2$ ), but MFC-2 (232.1 mV/decade) obtained a higher anode slope than MFC-1 (181.4 mV/decade) and MFC-3 (206.9 mV/decade).

**Table 3.** The exchange current densities ( $i_0$ ) and anodic slopes of the MFCs obtained from Tafel plots

Testing time	Reactor	$i_0$ (mA/cm <sup>2</sup> )	Anode slope $RT/\eta F$ (mV/decade)
After 10 days of operation	MFC-1	0.133	181.4
	MFC-2	0.172	232.1
	MFC-3	0.038	206.9
After 55 days of operation	MFC-1	0.123	192.3
	MFC-2	0.174	398.6
	MFC-3	0.015	171.6

The general trend of exchange current density was consistent with the CV results (Fig. 4a), because the CV curves obtained were at the higher overpotentials than Tafel curves. Higher exchange current density implies faster reaction rate and more effective utilization of the electrons [25], but higher Tafel slope indicates the requirement of higher activation energy that makes the reaction less favorable [22]. After 55 days of operation with the HMWG hydrolysate as the fuel (Fig. 5b), the exchange current densities of MFC-1 and MFC-3 decreased to 0.123 mA/cm<sup>2</sup> and 0.015 mA/cm<sup>2</sup>, corresponding to 7.5% and 60.5% lower than the values obtained after 10 days of operation. But for MFC-2, there was no obvious difference in its exchange current density. The anode slopes of MFC-1 and MFC-2 increased to 192.3 mV/decade and 398.6 mV/decade, respectively. However, the anode slope of MFC-3 declined from 206.9 mV/decade to 171.6 mV/decade. These results proved that the HMWG hydrolysate with high concentration restrained the bioelectrocatalytic activities of the anode biofilms similarly.

#### 3.4. SEM images of the anode biofilms

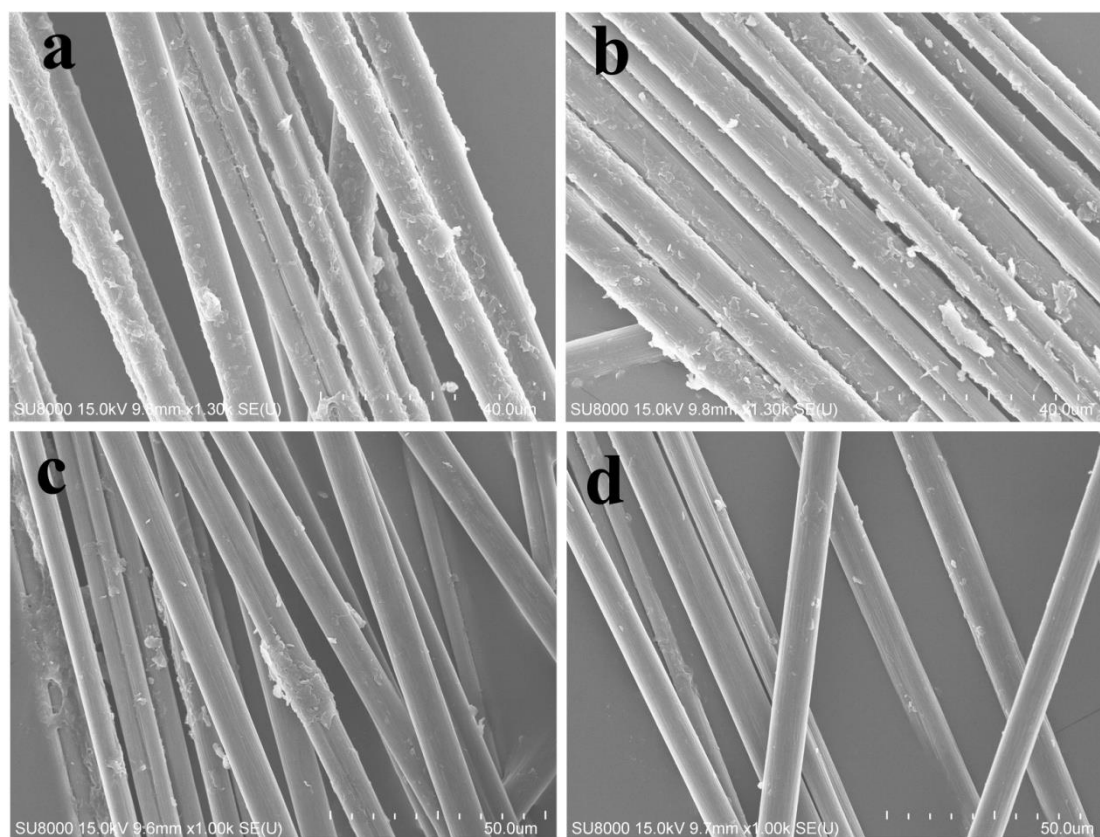


**Figure 6.** SEM images of the anode biofilms after the experiments finished. (a) MFC-1, (b) MFC-2, (c) MFC-3, (d) bare electrode

The anode biofilms of the MFCs were examined by SEM after the experiments finished. Each graphite fibre of bare electrode had a relatively smooth surface and an average diameter of about 8  $\mu\text{m}$  (Fig. 6d). Large quantity of microorganisms were observed on the anode surfaces of MFC-1 (Fig. 6a) and MFC-2 (Fig. 6b). However, only few bacteria were adhered on the anode surface of MFC-3, and these microbes were compactly agglomerated (Fig. 6c). These implies that the decreased electrocatalytic activities of the MFC-3 anode after long-term operation was mainly ascribed to the attenuated microorganisms on its surface.

#### 4. DISCUSSION

Microbial fuel cells hold great potential in extracting energy from organic waste. Heavy metal-containing organic waste was first explored as the fuel for MFCs in this study. MFCs with the HMWG hydrolysate as the fuel achieved CEs of 11.5–15.7%, which were comparable to that ( $13.4 \pm 0.3\%$ ) achieved in another study, where lactic acid was used as the fuel for the similar MFC reactor [26]. The MPDs of the MFCs with the HMWG hydrolysate could get up to 381  $\text{mW}/\text{m}^2$ , which was still much lower than that obtained in a membrane-less single chamber MFC with the same size using cellulose as the fuel in another report [27]. From the results of polarization and power curves, the MPDs of the MFCs reduced with the increase of the concentration of the HMWG hydrolysate. This phenomenon was inconsistent with the results in other reports [13, 28, 29], where the power densities of MFCs increased with the increase of the organic loads. It can be speculated that heavy metals in the HMWG hydrolysate had played important roles in power generation of the MFCs. The decreased power density after long-term operation was ascribed to the declined anode performance, which could be summarized from the results of the anode and cathode polarization curves, CV and Tafel tests.

Certain heavy metals are toxic to the metabolism of microorganisms or activity of enzyme, including  $\text{Cu}^{2+}$ ,  $\text{Hg}^{2+}$ ,  $\text{Cd}^{2+}$ ,  $\text{Pb}^{2+}$  and  $\text{Cr}_2\text{O}_7^-$ , which can lead to negative effect on the performance of MFCs [30]. The toxicity of heavy metals is related to their concentration. Heavy metals with high concentration, such as  $\text{Cd}^{2+}$  of 300  $\mu\text{M}$  [31],  $\text{Cu}^{2+}$  of 15.0  $\text{mg}/\text{L}$  [32] and  $\text{Zn}^{2+}$  of 500  $\mu\text{M}$  [31], would cause a rapid voltage drop of MFC. These reports all utilized synthetic wastewater as the fuel and only one or two kinds of heavy metals were involved. The HMWG hydrolysate in this study contained several kinds of heavy metals, although their concentration were at the level of micrograms per liter. The gradually voltage drops were observed in MFCs with different concentrations of the HMWG hydrolysate. However, low concentrations of the HMWG hydrolysate had slight influences on the electrocatalytic activities of the MFC anode (MFC-1 and MFC-2), which might because that microbial communities could adaptively change with the kinds and concentrations of heavy metals [32, 33]. Heavy metals in the higher concentrations of the HMWG hydrolysate (MFC-3) might inhibit the grows

and reproduction of microorganisms, resulting in a decrease in cell density and species richness [34], which could be seen from the SEM images (Fig. 6).

To achieve stable and sustainable electricity generation from heavy metal-containing organic wastes in MFCs, efforts should be taken to alleviate the toxicity of heavy metals to anode biofilms, like heavy metal removal through pretreatment or adding a complexing agent. It is noteworthy that the HMWG used in this work was first liquefied by a thermal hydrolysis process, which would offset a quantity of energy produced by MFCs. Thus, further research will be focused on using solid HMWG powder as the fuel for MFCs directly, and the process should be investigated in detail, including the hydrolytic acidification of the HMWG, the releasing rule of heavy metals, the evolution of microbial community structure and long-term stability.

## 5. CONCLUSIONS

The HMWG hydrolysate was used as the fuel for MFCs. The maximum coulombic efficiency and power density got up to 15.7% and 381 mW/m<sup>2</sup>, and the corresponding removal rate of chemical oxygen demand was 83.4%. High concentration of the HMWG hydrolysate restrained electricity production in a MFC, especially after long-terms of operation. The decreased performance in electricity generation was mainly ascribed to the declined electrocatalytic activities of the MFC anode and the attenuated microorganisms on its surface. Attention should be paid to the toxicity of heavy metals in energy recovery from heavy metal-containing organic wastes by MFCs.

E-supplementary data of this work can be found in online version of the paper.

## ACKNOWLEDGEMENTS

We acknowledge the financial support from the National Natural Science Foundation of China (No. 51508167 and 51604099) and Foundation of Henan Educational Committee (No. 18A610001 and 17A610007).

## References

1. A.Lu, J. Wang, X. Qin, K. Wang, P. Han, S. Zhang, *Sci. Total Environ.*, 425 (2012) 66.
2. J. Zhang, H. Li, Y. Zhou, L. Dou, L. Cai, L. Mo, J. You, *Environ. Pollut.*, 235 (2018) 710.
3. B. Liu, S. Ai, W. Zhang, D. Huang, Y. Zhang, *Sci. Total Environ.*, 609 (2017) 822.
4. A. Singh, R.K. Sharma, M. Agrawal, F.M. Marshall, *Food Chem. Toxicol.*, 48 (2010) 611.
5. J. Lee, J.R. Kim, S. Jeong, J. Cho, J.Y. Kim, *Waste Manag.*, 59 (2017) 498.
6. P.L. McCarty, J. Bae, J. Kim, *Environ. Sci. Technol.*, 45 (2011) 7100.
7. M. Sun, L.-F. Zhai, W.-W. Li, H.-Q. Yu, *Chem. Soc. Rev.*, 45 (2016) 2847.
8. P. Pandey, V.N. Shinde, R.L. Deopurkar, S.P. Kale, S.A. Patil, D. Pant, *Appl. Energ.*, 168 (2016) 706.
9. S.K. Chaudhuri, D.R. Lovley, *Nat. Biotechnol.*, 21 (2003) 1229.
10. Z. Ren, T.E. Ward, J.M. Regan, *Environ. Sci. Technol.*, 41 (2007) 4781.
11. Z. Liu, J. Liu, S. Zhang, Z. Su, *Biochem. Eng. J.*, 45 (2009) 185.
12. H. Liu, R. Ramnarayanan, B.E. Logan, *Environ. Sci. Technol.*, 38 (2004) 2281.
13. M.A. Jablonska, M.K. Rybarczyk, M. Lieder, *Bioresource Technol.*, 208 (2016) 117.
14. Z. Liu, Y. He, R. Shen, Z. Zhu, X.H. Xing, B. Li, Y. Zhang, *Bioresource Technol.*, 185 (2015) 294.
15. S.H.A. Hassan, S.M.F. Gad El-Rab, M. Rahimnejad, M. Ghasemi, J.-H. Joo, Y. Sik-Ok, I.S. Kim,

- S.-E. Oh, *Int. J. Hydrogen Energ.*, 39 (2014) 9490.
16. K.P. Gregoire, J.G. Becker, *Bioresource Technol.*, 119 (2012) 208.
  17. W. Miran, M. Nawaz, J. Jang, D.S. Lee, *Sci. Total Environ.*, 547 (2016) 197.
  18. S. Cheng, B.E. Logan, *Electrochem. Commun.*, 9 (2007) 492.
  19. B.E. Logan, B. Hamelers, R. Rozendal, U. Schröder, J. Keller, S. Freguia, P. Aelterman, W. Verstraete, K. Rabaey, *Environ. Sci. Technol.*, 40 (2006) 5181.
  20. Y. Feng, X. Wang, B.E. Logan, H. Lee, *Appl. Microbiol. Biotechnol.*, 78 (2008) 873.
  21. APHA, Standard Methods for the Examination of Water and Wastewater, Twenty ed., American Public Health Association, (2005) Washington, DC, USA.
  22. S.V. Raghavulu, J.A. Modestra, K. Amulya, C.N. Reddy, S. Venkata Mohan, *Bioresource Technol.*, 146 (2013) 696.
  23. S. Srikanth, S. Venkata Mohan, *Bioresource Technol.*, 119 (2012) 241.
  24. F. Zhao, R.C.T. Slade, J.R. Varcoe, *Chem. Soc. Rev.*, 38 (2009) 1926.
  25. B. Ge, K. Li, Z. Fu, L. Pu, X. Zhang, Z. Liu, K. Huang, *J. Power Sources*, 303 (2016) 325.
  26. P.D. Kiely, G. Rader, J.M. Regan, B.E. Logan, *Bioresource Technol.*, 102 (2011) 361.
  27. S. Cheng, P. Kiely, B.E. Logan, *Bioresource Technol.*, 102 (2011) 367.
  28. A. Tremouli, G. Antonopoulou, S. Bebelis, G. Lyberatos, *Bioresource Technol.*, 131 (2013) 380.
  29. Y. Feng, X. Wang, B.E. Logan, H. Lee, *Biotechnol.*, 78 (2008) 873.
  30. Z. Lu, D. Chang, J. Ma, G. Huang, L. Cai, L. Zhang, *J. Power Sources*, 275 (2015) 243.
  31. C. Abourached, T. Catal, H. Liu, *Water Res.*, 51 (2014) 228.
  32. Y. Wu, X. Zhao, M. Jin, Y. Li, S. Li, F. Kong, J. Nan, A. Wang, *Bioresource Technol.*, 253 (2018) 372.
  33. L. Huang, Q. Wang, L. Jiang, P. Zhou, X. Quan, B.E. Logan, *Environ. Sci. Technol.*, 49 (2015) 9914.
  34. I. Kamika, M.N.B. Momba, *Sci. Total Environ.*, 410-411 (2011) 172